PROCEEDINGS OF SCIENCE

Lattice QCD calculation of form factors for $\Lambda_b \to \Lambda(1520)\ell^+\ell^-$ decays

Stefan Meinel*
Department of Physics, University of Arizona, Tucson, AZ 85721, USA
RIKEN BNL Research Center, Brookhaven National Laboratory, Upton, NY 11973, USA
E-mail: smeinel@email.arizona.edu

Gumaro Rendon
Department of Physics, University of Arizona, Tucson, AZ 85721, USA
E-mail: jgrs@email.arizona.edu

Experimental results for mesonic $b \to s\mu^+\mu^-$ decays show a pattern of deviations from Standard-Model predictions, which could be due to new fundamental physics or due to an insufficient understanding of hadronic effects. Additional information on the $b \to s\mu^+\mu^-$ transition can be obtained from Λ_b decays. This was recently done using the process $\Lambda_b \to \Lambda\mu^+\mu^-$, where the Λ is the lightest strange baryon. A further interesting channel is $\Lambda_b \to p^+K^-\mu^+\mu^-$, where the p^+K^- final state receives contributions from multiple higher-mass Λ resonances. The narrowest and most prominent of these is the $\Lambda(1520)$, which has $J^P = \frac{3}{2}^-$. Here we present an ongoing lattice QCD calculation of the relevant $\Lambda_b \to \Lambda(1520)$ form factors. We discuss the choice of interpolating field for the $\Lambda(1520)$, and explain our method for extracting the fourteen $\Lambda_b \to \Lambda(1520)$ helicity form factors from correlation functions that are computed in the $\Lambda(1520)$ rest frame. We present preliminary numerical results at a pion mass of 340 MeV and a lattice spacing of 0.11 fm. This calculation uses a domain-wall action for the u, d, and s quarks and a relativistic heavy-quark action for the b quark, and is based on gauge-field configurations generated by the RBC and UKQCD Collaborations.

34th annual International Symposium on Lattice Field Theory
24-30 July 2016
University of Southampton, UK

*Speaker.

© Copyright owned by the author(s) under the terms of the Creative Commons Attribution-NonCommercial-NoDerivatives 4.0 International License (CC BY-NC-ND 4.0).

arXiv:1608.08110v3 [hep-lat] 20 Mar 2017

1. Introduction

Flavor-changing neutral-current decays of bottom hadrons play an important role in the search for physics beyond the Standard Model. The effective Hamiltonian describing $b \to s\ell^+\ell^-$ decays at low energies [1] contains the operators

$$O_{7(7')} = \frac{m_b}{e}\bar{s}\sigma^{\mu\nu}P_{R(L)}b\,F_{\mu\nu}, \quad O_{9(9')} = \bar{s}\gamma_\mu P_{L(R)}b\,\bar{\ell}\gamma^\mu\ell, \quad O_{10(10')} = \bar{s}\gamma_\mu P_{L(R)}b\,\bar{\ell}\gamma^\mu\gamma_5\ell, \tag{1.1}$$

as well as four-quark and gluonic operators. The Wilson coefficients C_i of these operators encode the short-distance physics and can be computed perturbatively in the Standard Model and in various new-physics scenarios. The values of C_i can also be constrained by fitting the decay rates and angular distributions measured in experiments, provided that the relevant hadronic matrix elements are known. Global analyses of experimental data for mesonic $b \to s\mu^+\mu^-$ decays, which use a combination of several theoretical methods [including lattice QCD for $O_{7(7')}$, $O_{9(9')}$, and $O_{10(10')}$], yield best-fit values for C_9 that are approximately 25% below the Standard-Model prediction (see, e.g., Refs. [2, 3, 4, 5]). However, the results for C_9 also depend on nonlocal matrix elements involving the four-quark operators O_1 and O_2, which are enhanced by charmonium resonances, and the approximations used for these matrix elements need further scrutiny.

In addition to the commonly studied B and B_s decays, the $b \to s\ell^+\ell^-$ couplings can also be probed in decays of Λ_b baryons (see Table 1 for a comparison of the most important semileptonic decay modes). Recently, the authors of Ref. [15] included, for the first time, the LHCb results for the differential branching fraction and three angular observables of the decay $\Lambda_b \to \Lambda(\to p^+\pi^-)\,\mu^+\mu^-$ [16] in an analysis of the Wilson coefficients $C_{9,9',10,10'}$. From a theoretical point of view [14, 17], this decay combines the best aspects of $B \to K\ell^+\ell^-$ (having only a single QCD-stable hadron in the final state, which simplifies the lattice QCD calculation of the form factors) and $B \to K^*(\to K\pi)\ell^+\ell^-$ (providing a large number of observables that give full sensitivity to all Dirac structures in the effective Hamiltonian). The fits performed in Ref. [15] prefer a positive shift in C_9, contrary to previous fits of only mesonic decays. This behavior could hint at large duality violations in the high-q^2 operator product expansion that is used to approximate the nonlocal matrix elements of O_1 and O_2. Unfortunately, the statistical uncertainties in the $\Lambda_b \to \Lambda(\to p^+\pi^-)\,\mu^+\mu^-$ data [16] are still quite large. One experimental challenge with this decay is that the hadron in the final state, the lightest Λ baryon, is electrically neutral and long-lived. It is therefore worth exploring decays proceeding through unstable Λ^* resonances, which can immediately decay into charged

	Probes all Dirac structures	Final hadron QCD-stable	Charged hadrons from b-decay vertex	LQCD Refs.
$B^+ \to K^+\ell^+\ell^-$	×	✓	✓	[6, 7, 8, 9]
$B^0 \to K^{*0}(\to K^+\pi^-)\ell^+\ell^-$	✓	×	✓	[10, 11, 12]
$B_s \to \phi(\to K^+K^-)\ell^+\ell^-$	✓	×	✓	[10, 11, 12]
$\Lambda_b^0 \to \Lambda^0(\to p^+\pi^-)\,\ell^+\ell^-$	✓	✓	×	[13, 14, 15]
$\Lambda_b^0 \to \Lambda^{*0}(\to p^+K^-)\,\ell^+\ell^-$	✓	×	✓	This work

Table 1: Comparison of exclusive $b \to s\ell^+\ell^-$ decay channels.

particles such as p^+K^- and produce tracks in the particle detectors that originate from the b-decay vertex.

The p^+K^--invariant-mass distribution in $\Lambda_b \to p^+K^-\mu^+\mu^-$ decays is expected to be similar to that in $\Lambda_b \to p^+K^- J/\psi$. As can be seen in Fig. 3 of Ref. [18], a large number of Λ^* resonances contribute to this decay in overlapping mass regions. However, one resonance produces a narrow peak that clearly stands out above the other contributions: the $\Lambda(1520)$, which is the lightest resonance with $J^P = \frac{3}{2}^-$. The $\Lambda(1520)$ has a width of 15.6 ± 1.0 MeV [19] and appears in the coupled channels pK, $\Sigma\pi$, $\Lambda\pi\pi$, and, less importantly, $\Sigma\pi\pi$. Given the small width, a naive analysis in which the $\Lambda(1520)$ is treated as if it were QCD-stable is expected to be quite accurate, and is therefore justified in a first lattice QCD calculation of $\Lambda_b \to \Lambda(1520)$ form factors. When working in the $\Lambda(1520)$ rest frame, the lowest energy level in the finite lattice volume can be identified with the resonance in the narrow-width approximation; in the rest frame, the pK, $\Sigma\pi$, $\Lambda\pi\pi$, and $\Sigma\pi\pi$ scattering-like states will appear at higher energies due to the nonzero back-to-back momenta required for a coupling to $J^P = \frac{3}{2}^-$.

In the following, we will use the notation Λ^* to refer to the $\Lambda(1520)$. The $\Lambda_b \to \Lambda^*$ matrix elements of the $b \to s$ vector, axial vector, and tensor currents [as needed for $O_{7(7')}$, $O_{9(9')}$, and $O_{10(10')}$] are described by 14 form factors [20]. Following the approach of Ref. [21], we have derived a new helicity-based definition of the $\Lambda_b \to \Lambda^*$ form factors. The decomposition for the vector current reads

$$\begin{aligned}
&\langle \Lambda^*(p',s')|\,\bar{s}\gamma^\mu b\,|\Lambda_b(p,s)\rangle \\
&= \bar{u}_\lambda(p',s')\Bigg[f_0\,\frac{(m_{\Lambda_b}-m_{\Lambda^*})\,p^\lambda q^\mu}{m_{\Lambda_b}\,q^2} + f_+\,\frac{(m_{\Lambda_b}+m_{\Lambda^*})\,p^\lambda (q^2(p^\mu+p'^\mu)-(m_{\Lambda_b}^2-m_{\Lambda^*}^2)q^\mu)}{m_{\Lambda_b}\,q^2\,s_+} \\
&\qquad + f_\perp\left(\frac{p^\lambda\gamma^\mu}{m_{\Lambda_b}} - \frac{2\,p^\lambda(m_{\Lambda_b}p'^\mu + m_{\Lambda^*}p^\mu)}{m_{\Lambda_b}\,s_+}\right) \\
&\qquad + f_{\perp'}\left(\frac{p^\lambda\gamma^\mu}{m_{\Lambda_b}} - \frac{2\,p^\lambda p'^\mu}{m_{\Lambda_b}m_{\Lambda^*}} + \frac{2\,p^\lambda(m_{\Lambda_b}p'^\mu + m_{\Lambda^*}p^\mu)}{m_{\Lambda_b}\,s_+} + \frac{s_-\,g^{\lambda\mu}}{m_{\Lambda_b}m_{\Lambda^*}}\right)\Bigg]u(p,s),
\end{aligned} \tag{1.2}$$

where $q = p - p'$, $s_\pm = (m_{\Lambda_b} \pm m_{\Lambda^*})^2 - q^2$, and the form factors f_0, f_+, $f_\perp$, $f_{\perp'}$ are functions of q^2. Above, $\bar{u}_\lambda(p',s')$ is the Rarita-Schwinger spinor for the Λ^*. Similar relations are obtained for the currents $\bar{s}\gamma^\mu\gamma_5 b$ (form factors g_0, g_+, $g_\perp$, $g_{\perp'}$), $\bar{s}i\sigma^{\mu\nu}q_\nu b$ (form factors h_+, $h_\perp$, $h_{\perp'}$), and $\bar{s}i\sigma^{\mu\nu}\gamma_5 q_\nu b$ (form factors $\widetilde{h}_+$, $\widetilde{h}_\perp$, $\widetilde{h}_{\perp'}$).

2. Interpolating field for the $\Lambda(1520)$

We work in the $\Lambda(1520)$ rest frame to allow an exact projection to the $J^P = \frac{3}{2}^-$ quantum numbers, and also for the reasons discussed in Sec. 1. In a first (unsuccessful) attempt at calculating the form factors, we used the interpolating field

$$\Lambda^{(\text{old})}_{j\gamma} = \varepsilon^{abc}\,(C\gamma_j)_{\alpha\beta}\,\left(\tilde{u}^a_\alpha\,\tilde{s}^b_\beta\,\tilde{d}^c_\gamma - \tilde{d}^a_\alpha\,\tilde{s}^b_\beta\,\tilde{u}^c_\gamma\right), \tag{2.1}$$

which has isospin 0 as required, and which we projected to $J^P = \frac{3}{2}^-$ by contracting with $P^{kj} = \left(g^{kj} - \frac{1}{3}\gamma^k\gamma^j\right)\frac{1-\gamma_0}{2}$ (above, the tilde on the quark fields denotes gauge-covariant Gaussian smearing).

$N_s^3 \times N_t$	β	$am_{u,d}^{(\mathrm{sea})}$	$am_s^{(\mathrm{sea})}$	$am_{u,d}^{(\mathrm{val})}$	$am_s^{(\mathrm{val})}$	a [fm]
$24^3 \times 64$	2.13	0.005	0.04	0.005	0.0323	0.1106(3)

m_π [MeV]	m_K [MeV]	m_N [MeV]	m_Λ [MeV]	m_Σ [MeV]
340(1)	550(2)	1168(5)	1272(5)	1320(6)

Table 2: Lattice parameters and preliminary results for selected hadron masses. Details on the lattice actions and ensemble generation can be found in Ref. [22]. We use all-mode-averaging (AMA) [23] with 1 exact and 32 sloppy measurements per configuration.

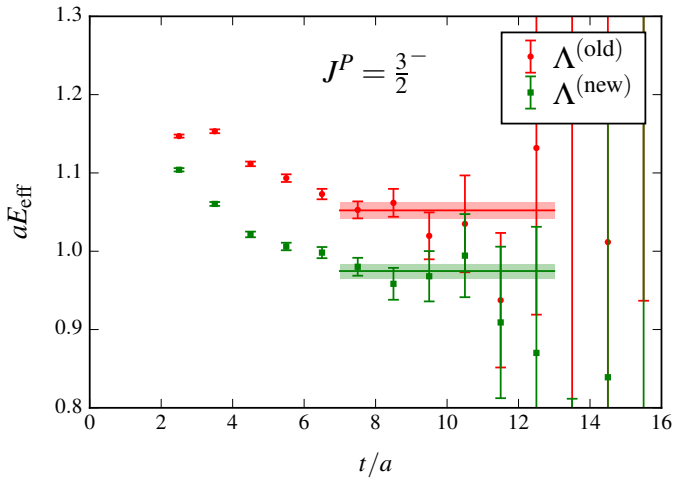

Figure 1: Effective-energy plot for the two-point functions computed with the interpolating fields defined in Eqs. (2.1) and (2.2). The preliminary results shown here are from 311 configurations (with AMA). The energies obtained from the fits are 1878(19) MeV and 1740(17) MeV.

With the interpolating field $\Lambda_{j\gamma}^{(\mathrm{old})}$, the numerical results for the ratios of three-point and two-point functions used to extract the form factors were very noisy and did not show plateaus. We then noticed that a previous lattice QCD study of Λ-baryon spectroscopy using interpolating fields similar to Eq. (2.1) in fact did not find a $\Lambda(1520)$-like state [24], while the calculation of Ref. [25], which included interpolating fields with covariant derivatives, did. This can be understood from quark models, in which the $\Lambda(1520)$ dominantly has an $L = 1$, $S = 1/2$, and flavor-$SU(3)$ singlet structure [26], very different from Eq. (2.1). We therefore now use the interpolating field

$$\Lambda_{j\gamma}^{(\mathrm{new})} = \varepsilon^{abc}\,(C\gamma_5)_{\alpha\beta}\left[\tilde{s}_\alpha^a\,\tilde{d}_\beta^b\,(\nabla_j\tilde{u})_\gamma^c - \tilde{s}_\alpha^a\,\tilde{u}_\beta^b\,(\nabla_j\tilde{d})_\gamma^c + \tilde{u}_\alpha^a\,(\nabla_j\tilde{d})_\beta^b\,\tilde{s}_\gamma^c - \tilde{d}_\alpha^a\,(\nabla_j\tilde{u})_\beta^b\,\tilde{s}_\gamma^c\right], \qquad (2.2)$$

which matches the structure suggested by nonrelativistic quark models and has naturally negative parity, so that it can be projected to $J^P = \frac{3}{2}^-$ by contracting with $P^{kj} = \left(g^{kj} - \frac{1}{3}\gamma^k\gamma^j\right)\frac{1+\gamma_0}{2}$ (note the plus sign). In Eq. (2.2), covariant derivatives acting on the strange quark have been eliminated using "integration by parts" (which is possible only at zero momentum). Numerical results for the two-point functions, with the lattice parameters given in Table 2, are shown in Fig. 1. The two-point function of the new interpolating field (2.2) shows a plateau at an energy close to $m_N + m_K$ and $m_\Sigma + m_\pi$, as expected for the $\Lambda(1520)$, while the two-point function of the old interpolating

field (2.1) shows an apparent plateau at a significantly higher energy that is likely associated with one or more states that have a larger overlap with an $S = 3/2$, $SU(3)$-octet structure.

3. Extracting the form factors from ratios of three-point and two-point functions

To determine the $\Lambda_b \to \Lambda(1520)$ form factors, we compute three-point functions

$$C^{(3,\mathrm{fw})}_{j\gamma\delta}(\mathbf{p},\Gamma,t,t') = \sum_{\mathbf{y},\mathbf{z}} e^{-i\mathbf{p}\cdot(\mathbf{y}-\mathbf{z})} \left\langle \Lambda^{(\mathrm{new})}_{j\gamma}(x_0,\mathbf{x})\, J_\Gamma(x_0-t+t',\mathbf{y})\, \overline{\Lambda}_{b\delta}(x_0-t,\mathbf{z}) \right\rangle, \tag{3.1}$$

where $J_\Gamma = \rho_\Gamma \sqrt{Z_V^{(ss)} Z_V^{(bb)}}\, [\bar{s}\Gamma b + a\, d_1\, \bar{s}\Gamma \boldsymbol{\gamma}\cdot\boldsymbol{\nabla} b]$ is the renormalized and $\mathcal{O}(a)$-improved $b \to s$ current, $\Lambda_{b\delta} = \varepsilon^{abc}\,(C\gamma_5)_{\alpha\beta}\, \tilde{u}^a_\alpha\, \tilde{d}^b_\beta\, \tilde{b}^c_\delta$ is the interpolating field for the Λ_b, $\mathbf{p}$ is the momentum of the Λ_b, and t is the source-sink separation. The bottom quark is implemented with the relativistic heavy-quark action of Ref. [27]. Using also the time-reversed backward three-point function and the Λ^* and Λ_b two-point functions, we form the ratios

$$\mathscr{R}^{jk\mu\nu}(\mathbf{p},t,t')^X = \frac{\mathrm{Tr}\Big[P^{jl}\, C^{(3,\mathrm{fw})}_l(\mathbf{p},\Gamma^\mu_X,t,t')\, (\not{p}+m_{\Lambda_b})\, C^{(3,\mathrm{bw})}_m(\mathbf{p},\Gamma^\nu_X,t,t-t')\, P^{mk}\Big]}{\mathrm{Tr}\Big[P^{lm}\, C^{(2,\Lambda^*)}_{lm}(t)\Big]\, \mathrm{Tr}\Big[(\not{p}+m_{\Lambda_b})\, C^{(2,\Lambda_b)}(\mathbf{p},t)\Big]}, \tag{3.2}$$

where $X \in \{V, A, TV, TA\}$ and $\Gamma^\mu_V = \gamma^\mu$, $\Gamma^\mu_A = \gamma^\mu\gamma_5$, $\Gamma^\mu_{TV} = i\sigma^{\mu\nu}q_\nu$, $\Gamma^\mu_{TA} = i\sigma^{\mu\nu}\gamma_5 q_\nu$. We then contract with the timelike, longitudinal, and transverse polarization vectors

$$\varepsilon^{(0)} = (q^0, \mathbf{q}), \qquad \varepsilon^{(+)} = (|\mathbf{q}|, (q^0/|\mathbf{q}|)\mathbf{q}), \qquad \varepsilon^{(\perp,j)} = (0, \mathbf{e}_j \times \mathbf{q}) \tag{3.3}$$

as follows:

$$\mathscr{R}^X_0(\mathbf{p},t,t') = g_{jk}\, \varepsilon^{(0)}_\mu \varepsilon^{(0)}_\nu\, \mathscr{R}^{jk\mu\nu}(\mathbf{p},t,t')^X, \tag{3.4}$$

$$\mathscr{R}^X_+(\mathbf{p},t,t') = g_{jk}\, \varepsilon^{(+)}_\mu \varepsilon^{(+)}_\nu\, \mathscr{R}^{jk\mu\nu}(\mathbf{p},t,t')^X, \tag{3.5}$$

$$\mathscr{R}^X_\perp(\mathbf{p},t,t') = p_j\, p_k\, \varepsilon^{(\perp,l)}_\mu \varepsilon^{(\perp,l)}_\nu\, \mathscr{R}^{jk\mu\nu}(\mathbf{p},t,t')^X, \tag{3.6}$$

$$\mathscr{R}^X_{\perp'}(\mathbf{p},t,t') = \left[\varepsilon^{(\perp,m)}_j \varepsilon^{(\perp,m)}_k - \frac{1}{2}\, p_j\, p_k\right] \varepsilon^{(\perp,l)}_\mu \varepsilon^{(\perp,l)}_\nu\, \mathscr{R}^{jk\mu\nu}(\mathbf{p},t,t')^X. \tag{3.7}$$

Up to excited-state contamination that is suppressed at large time separations, these quantities are equal to the squares of the individual helicity form factors times known kinematic factors. For example, in the case of the vector current we obtain the helicity form factors by computing

$$R^V_0(\mathbf{p},t) = \sqrt{\frac{12 E_{\Lambda_b} m^2_{\Lambda_b}\, \mathscr{R}^V_0(\mathbf{p},t,t/2)}{(E_{\Lambda_b}-m_{\Lambda_b})(m_{\Lambda_b}-m_\Lambda)^2(E_{\Lambda_b}+m_{\Lambda_b})^2}} = f_0 + (\text{excited-state contribs.}), \tag{3.8}$$

$$R^V_+(\mathbf{p},t) = \sqrt{\frac{12 E_{\Lambda_b} m^2_{\Lambda_b}\, \mathscr{R}^V_+(\mathbf{p},t,t/2)}{(E_{\Lambda_b}+m_{\Lambda_b})(m_{\Lambda_b}+m_\Lambda)^2(E_{\Lambda_b}-m_{\Lambda_b})^2}} = f_+ + (\text{excited-state contribs.}), \tag{3.9}$$

$$R^V_\perp(\mathbf{p},t) = \sqrt{-\frac{9 E_{\Lambda_b} m^2_{\Lambda_b}\, \mathscr{R}^V_\perp(\mathbf{p},t,t/2)}{(E_{\Lambda_b}-m_{\Lambda_b})^4(E_{\Lambda_b}+m_{\Lambda_b})^3}} = f_\perp + (\text{excited-state contribs.}), \tag{3.10}$$

$$R^V_{\perp'}(\mathbf{p},t) = \sqrt{-\frac{2 E_{\Lambda_b} m^2_{\Lambda_b}\, \mathscr{R}^V_{\perp'}(\mathbf{p},t,t/2)}{(E_{\Lambda_b}-m_{\Lambda_b})^4(E_{\Lambda_b}+m_{\Lambda_b})^3}} = f_{\perp'} + (\text{excited-state contribs.}). \tag{3.11}$$

Preliminary numerical results for these quantities for all 14 helicity form factors at momentum $\mathbf{p} = (0,0,3)\frac{2\pi}{L}$ are shown in Fig. 2. Reasonably good signals are obtained for most form factors.

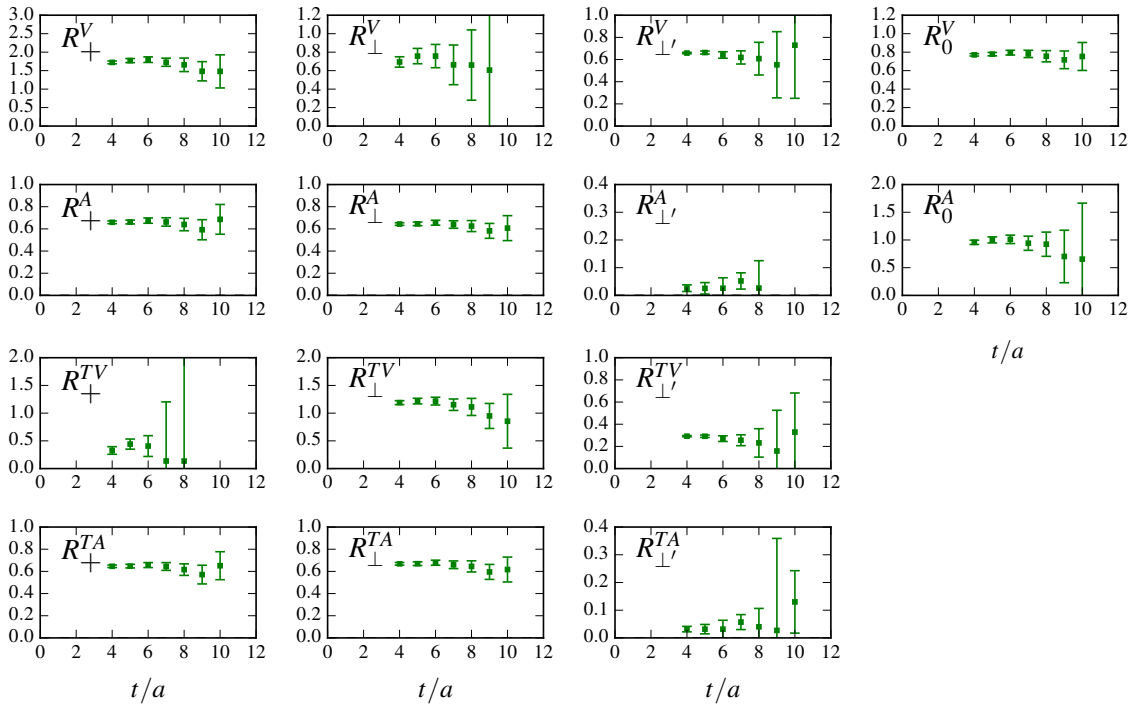

Figure 2: Preliminary results for the functions $R_i^X(\mathbf{p},t)$, defined in Eqs. (3.8)-(3.11) for the vector current and similarly for the other currents, at the Λ_b-momentum $\mathbf{p} = (0,0,3)\frac{2\pi}{L}$. These functions become equal to the $\Lambda_b \to \Lambda(1520)$ helicity form factors at the given momentum for large source-sink separation t. The results shown here are from 77 configurations (with AMA).

4. Next steps

The drawback of working in the $\Lambda(1520)$ rest frame is that very large Λ_b momenta are required to appreciably move q^2 away from $q^2_{\text{max}} = (m_{\Lambda_b} - m_{\Lambda^*})^2$, as illustrated in Fig. 3. With the relativistic heavy-quark action used so far, this introduces potentially large heavy-quark discretization errors. We therefore plan to perform additional calculations in which the b quark is implemented with moving NRQCD [28], which will allow us to reach much higher momenta. We also plan to substantially increase statistics and add two ensembles to study the lattice-spacing and light-quark-mass dependence of the results.

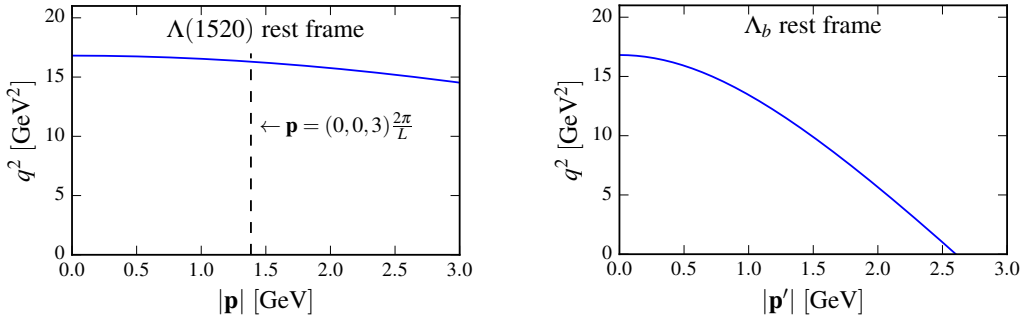

Figure 3: Value of q^2 as a function of the Λ_b momentum in the $\Lambda(1520)$ rest frame (left), and as a function of the $\Lambda(1520)$ momentum in the Λ_b rest frame (right).

Acknowledgments: This work is supported by National Science Foundation Grant Number PHY-1520996, and by the RHIC Physics Fellow Program of the RIKEN BNL Research Center. High-performance computing resources were provided by XSEDE (supported by National Science Foundation Grant Number OCI-1053575) and NERSC (supported by U.S. Department of Energy Grant Number DE-AC02-05CH11231).

References

[1] B. Grinstein, M. J. Savage, and M. B. Wise, Nucl. Phys. B **319**, 271 (1989).

[2] W. Altmannshofer and D. M. Straub, Eur. Phys. J. C **75**, 382 (2015).

[3] W. Altmannshofer and D. M. Straub, arXiv:1503.06199.

[4] S. Descotes-Genon, L. Hofer, J. Matias, and J. Virto, JHEP **1606**, 092 (2016).

[5] T. Hurth, F. Mahmoudi, and S. Neshatpour, Nucl. Phys. B **909**, 737 (2016).

[6] C. Bouchard *et al.* (HPQCD Collaboration), Phys. Rev. D **88**, 054509 (2013).

[7] C. Bouchard *et al.* (HPQCD Collaboration), Phys. Rev. Lett. **111**, 162002 (2013).

[8] J. A. Bailey *et al.* (Fermilab Lattice and MILC Collaborations), Phys. Rev. D **93**, 025026 (2016).

[9] D. Du *et al.* (Fermilab Lattice and MILC Collaborations), Phys. Rev. D **93**, 034005 (2016).

[10] R. R. Horgan, Z. Liu, S. Meinel, and M. Wingate, Phys. Rev. D **89**, 094501 (2014).

[11] R. R. Horgan, Z. Liu, S. Meinel, and M. Wingate, Phys. Rev. Lett. **112**, 212003 (2014).

[12] J. Flynn, A. Jüttner, T. Kawanai, E. Lizarazo, and O. Witzel (RBC and UKQCD Collaborations), PoS LATTICE **2015**, 345 (2016).

[13] W. Detmold, C.-J. D. Lin, S. Meinel, and M. Wingate, Phys. Rev. D **87**, 074502 (2013).

[14] W. Detmold and S. Meinel, Phys. Rev. D **93**, 074501 (2016).

[15] S. Meinel and D. van Dyk, Phys. Rev. D **94**, 013007 (2016).

[16] R. Aaij *et al.* (LHCb Collaboration), JHEP **1506**, 115 (2015).

[17] P. Böer, T. Feldmann, and D. van Dyk, JHEP **1501**, 155 (2015).

[18] R. Aaij *et al.* (LHCb Collaboration), Phys. Rev. Lett. **115**, 072001 (2015).

[19] K. A. Olive *et al.* (Particle Data Group Collaboration), Chin. Phys. C **38**, 090001 (2014).

[20] L. Mott and W. Roberts, Int. J. Mod. Phys. A **27**, 1250016 (2012).

[21] T. Feldmann and M. W. Y. Yip, Phys. Rev. D **85**, 014035 (2012).

[22] Y. Aoki *et al.* (RBC and UKQCD Collaborations), Phys. Rev. D **83**, 074508 (2011).

[23] E. Shintani, R. Arthur, T. Blum, T. Izubuchi, C. Jung, and C. Lehner, Phys. Rev. D **91**, 114511 (2015).

[24] G. P. Engel, C. B. Lang, and A. Schäfer (Bern-Graz-Regensburg Collaboration), Phys. Rev. D **87**, 034502 (2013).

[25] R. G. Edwards, N. Mathur, D. G. Richards, and S. J. Wallace (Hadron Spectrum Collaboration), Phys. Rev. D **87**, 054506 (2013).

[26] D. Gromes, Z. Phys. C **18**, 249 (1983).

[27] Y. Aoki *et al.* (RBC and UKQCD Collaborations), Phys. Rev. D **86**, 116003 (2012).

[28] R. R. Horgan *et al.*, Phys. Rev. D **80**, 074505 (2009).